Textile & Leather Review

ISSN 2623-6281| www.tlr-journal.com | 10.31881/TLR

Application of Plasma-Activated SiO_2-Epoxy Coated Functional Textile-Reinforced Composites in Building Structural Reinforcement

Guohua Cheng

How to cite: Cheng G. Application of Plasma-Activated SiO_2-Epoxy Coated Functional Textile-Reinforced Composites in Building Structural Reinforcement. Textile & Leather Review. 2026; 9:1210-1233. https://doi.org/10.31881/TLR.2026.1210

How to link: https://doi.org/10.31881/TLR.2026.1210

Published: 28 April 2026

Application of Plasma-Activated SiO_2-Epoxy Coated Functional Textile-Reinforced Composites in Building Structural Reinforcement

Guohua Cheng

China Railway Siyuan Srvey and Design Group Co., LTD, Wuhan 430061, Hubei, China

tsyjtcgh@163.com

Article

https://doi.org/10.31881/TLR.2026.1210

Received 12 September 2025; Accepted 23 October 2025; Published 28 April 2026

ABSTRACT

During long-term use in building structural reinforcement, conventional unmodified textile-reinforced composites (TRCs) often suffer from reduced bearing capacity and functional degradation due to bond failure between the fabric and concrete, making them unable to meet the durability and reliability requirements of modern building structures. This paper proposes a multifunctional composite reinforcement system integrating nano-modification with conductive textiles. Carbon fiber fabrics are plasma-treated and coated with a SiO_2-epoxy hybrid layer. These are then woven with stainless steel fibers into a smart grid, layered onto the bottom of concrete beams and impregnated with a modified cement matrix. After aging through hydrothermal cycles, flexural loading and electrical resistance monitoring are performed. Flexural tests on five replicate beams per group show the system effectively improves the structural flexural bearing capacity by over 105% compared to unreinforced beams. The degradation rate of the interfacial bond strength after aging is limited to 12%. The self-sensing sensitivity GF (Gauge Factor) exceeds 3.38, and the signal response is stable. The resulting multifunctional composite material combines high strength, durability, and functional monitoring, making it suitable for building reinforcement projects in long-term service environments.

KEYWORDS

building structural reinforcement, textile-reinforced composites, nano-modified coatings, conductive mesh, bonding stability

INTRODUCTION

Building structures often face problems such as degraded bearing capacity, crack expansion, and reduced durability during long-term service. The adoption of efficient, durable, and functionally responsive reinforcement technologies has become a key path to ensuring infrastructure safety. In recent years, textile-reinforced composites, due to their advantages such as light weight, high strength, designability, and ease of construction, have gradually replaced traditional steel plate reinforcement and are widely used to improve the performance of components such as beams, slabs, and columns [1,2]. However, existing material systems are prone to bond failure between the fabric and concrete under complex environmental conditions, resulting in delamination of the reinforcement layer and a significant degradation of mechanical properties [3,4]. Furthermore, most materials only have a single reinforcement function and lack the ability to provide real-time feedback on the structural state, resulting in significant shortcomings in long-term monitoring and early warning [5,6]. The mechanisms of material performance degradation under environmental conditions such as humidity, heat, and freeze-thaw remain unclear, and effective technical paths for synergistically improving functional integration and structural stability remain lacking.

In recent years, research on functional textile composites has mainly focused on improving structural reinforcement performance. Elnassar Z et al. systematically analyzed the experimental results of FRCM (Fabric Reinforced Cementitious Matrix) reinforced concrete columns and pointed out that it could significantly improve bearing capacity and ductility, especially in terms of earthquake resistance and fire resistance. The combination of PBO (Poly-p-phenylene benzobisoxazole) fiber and modified high-strength mortar has the best performance. The material effect was affected by the strength of concrete, the number of FRCM layers, and the cross-sectional shape. The reinforcement response of low-strength or small-sized columns was more obvious [7]. Askouni P D et al. found that TRAAM (Textile-reinforced Alkali-Activated Mortar) is comparable to traditional TRM (Textile-reinforced Mortar) in bending, shear, compression, and earthquake resistance, and has environmental advantages, but its long-term durability and standardization system have not yet been established [8]. The application of different matrices has expanded the application range of materials, but the aging behavior lacks systematic data support. Wu C et al. summarized the application of TRC (Textile reinforced concrete) in building structures, emphasizing its lightweight, thin, and high-efficiency characteristics, while also having good freeze-thaw, chemical, and fire resistance [9]. The

stability of the material in complex environments has been preliminarily verified, but the functional integration capability has not been deeply explored. Karakasis I C et al. pointed out that TRM can effectively inhibit carbonization and chloride ion penetration, but the erosion diffusion mechanism changes with the chemical evolution of the material, and there is uncertainty in the protective performance [10]. Escobar K I et al. found through multi-scale experiments that the cracking behavior and bonding performance of hemp fiber TRM are significantly affected by the reinforcement rate and mortar type. The failure mode is mainly concrete crushing accompanied by local debonding, and bonding failure becomes the key factor limiting the performance [11]. Existing research generally focuses on single mechanical enhancement or short-term protective effects, and lacks an effective solution to the problem of synergistic degradation of bonding degradation and functional stability in long-term service.

The control and sensing integration technology of the bonding interface between fabric and matrix materials is gradually being applied in textile-reinforced composite materials. Preinstorfer P et al. systematically analyzed the multi-level factors affecting the bonding performance of TRC, covering fiber, matrix, fabric structure, and process parameters, and provided a theoretical basis for interface optimization [12]. Material performance depends on the synergistic effect between the components, and the interface design needs to take into account both mechanical and process requirements. Joo J H et al. summarized the surface modification technology of carbon fiber and pointed out that oxidation, coating, plasma treatment, and other methods can significantly improve the adhesion between fiber and matrix, which is suitable for polymer-based systems, but has limited adaptability to alkaline cement environments [13]. Different modification strategies affect the stability of the interface, and environmental durability becomes a key constraint for practical application. Elseady A A E et al. proposed a self-sensing technology based on two-dimensional carbon fiber fabrics, and monitored the cracking and fiber slip behavior of TRC in real-time through a sensor network. It was found that the matrix quality and fiber orientation directly affected the sensing sensitivity [14]. Functional realization depends on the integrity of the conductive path, and structural deformation and signal response need to be synchronized. Embedding the conductive network into the interlayer interface to achieve integrated integration of electrodes and pathways is conducive to simplifying the manufacturing process and improving designability [15]. The integration method overcomes the difficulties of filler dispersion and electrode connection, but the coupled degradation of conductivity and bonding properties

during long-term service is not considered. Singh S et al. embedded graphene oxide-coated glass fiber as a piezoresistive sensor into GFRC (Glass Fiber Reinforced Cement). The three-point bending test showed that it can effectively respond to strain and damage evolution. The application of functional phase enhances the structural sensing ability, but the stability of the coating in alkaline environment limits its durable application [16]. Although existing research has achieved improvements in sensing and interface, it has mostly focused on single performance improvement and lacks a systematic design for the coordinated durability of function and structure under complex environmental conditions.

Based on the above research status and analysis, this paper proposes a composite reinforcement system that integrates structural reinforcement and self-sensing capabilities to address key issues such as significant bond degradation, limited functionality, and a lack of real-time monitoring capabilities during long-term service. The carbon fiber fabric surface is plasma-treated to increase the density of active groups, significantly improving the chemical bonding between the fiber and the cement matrix. Subsequently, a hybrid coating composed of nano-SiO_2 and epoxy resin is sprayed to form a reinforced bonding layer, aiming to overcome the problem of interfacial degradation in hot and humid environments. Stainless steel fibers and treated carbon fibers are mixed in a specific ratio to form a conductive mesh, achieving the dual functions of mechanical reinforcement and strain self-sensing. The mesh is embedded in a modified cement matrix in three layers and adhered layer by layer to the tensile zone of the concrete component, achieving multi-layer protection and functional integration. A polymer emulsion is applied into the material system to adjust the matrix toughness and optimize the stress transfer path between the fiber and matrix, significantly improving the bond stability and crack control between the reinforcement layer and the original structure. By combining structural design with material modification, a stable response relationship between strain and electrical resistance change is established, providing a data foundation for structural health monitoring and overcoming the limitations of traditional materials' single functions.

MATERIAL DESIGN AND PREPARATION OF MULTIFUNCTIONAL TEXTILE COMPOSITE REINFORCEMENT SYSTEMS

Figure 1 illustrates the systematic construction framework for functional textile-reinforced composites, from material components to multi-scale structures and comprehensive performance outputs, demonstrating the progressive relationships and key innovations at each level.

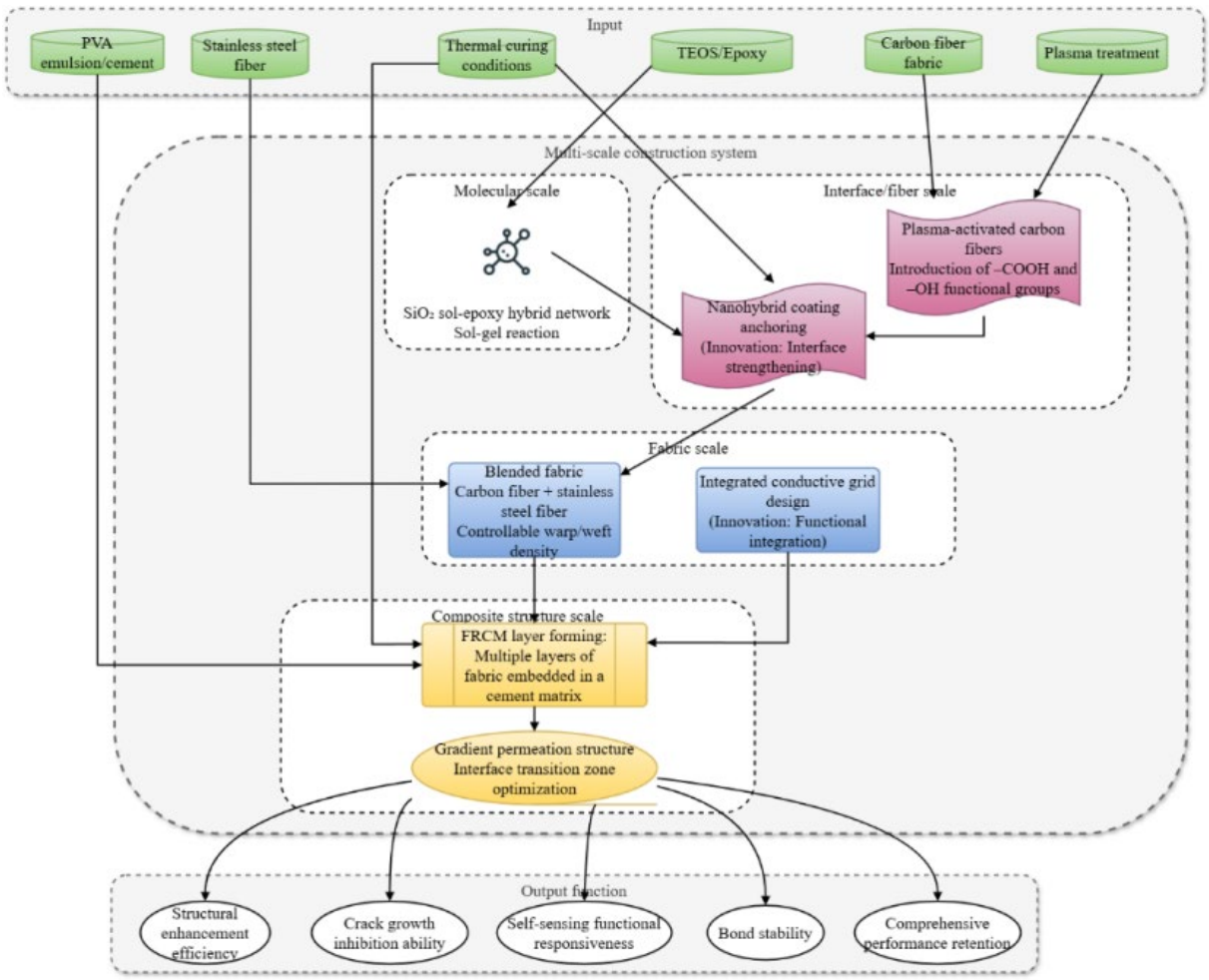

Figure 1. Multi-scale construction framework for multifunctional textile composite systems

Figure 1 systematically illustrates the multi-scale construction pathway for multifunctional textile composite systems. Raw materials and process conditions serve as inputs to drive system formation. Carbon fiber fabrics are plasma-treated to apply reactive functional groups. These interact synergistically with the SiO_2 sol-epoxy hybrid network generated by the hydrolysis of TEOS (Tetraethyl Orthosilicate) to form a reinforced interface

layer at the fiber scale, achieving chemical anchoring and stress buffering. At the fabric scale, stainless steel fibers and carbon fibers are plain-woven to create a conductive mesh, integrating mechanical load-bearing and electrical response. This structure, combined with a modified cement matrix, forms a multilayered FRCM system at the composite scale. Gradient infiltration of the slurry optimizes the interfacial transition zone. Each level progresses from the molecular to the macroscopic, with input parameters acting on the two innovative nodes of interface reinforcement and functional integration. Ultimately, the outputs include comprehensive properties such as structural reinforcement, crack control, self-sensing response, and bond stability. This fully reveals the inherent connection between material design, structural preparation, and performance realization.

Surface Plasma Activation and Interface Modification of Carbon Fiber Fabrics

Carbon fiber fabrics are treated with atmospheric pressure plasma activation to improve their surface energy and chemical activity and enhance the adhesion of subsequent coatings [17,18]. This step is a key prerequisite for achieving subsequent efficient interface modification. The fabric is placed in a dielectric barrier discharge device with an electrode spacing of 5 mm. An alternating voltage with a frequency of 10 kHz and a power density of 1.8 W/cm² is applied. High-purity argon is applied as the working gas, and the gas flow rate is precisely controlled by a mass flow meter. Under normal pressure, the plasma jet uniformly irradiates the fabric surface. During the treatment, active particles bombard the fiber surface, etching micropores and applying polar functional groups such as carboxyl (–COOH) and hydroxyl (–OH) [19]. The changes in the surface chemical state are verified by XPS (X-ray Photoelectron Spectroscopy), and contact angle measurement is used to characterize the wettability improvement effect. During the plasma activation treatment process, to quantify the effect of energy input on the fiber surface modification effect, the specific energy density (SED) per unit area is applied as a key process control parameter, and its expression is:

$$\mathrm{SED}=\frac{P\cdot t}{A} \tag{1}$$

In Formula (1), P is the applied discharge power; t is the treatment time; A is the effective area of plasma action; the unit of SED is J/cm². This parameter comprehensively reflects the energy deposition level of the

plasma on the material per unit area, and directly affects the surface etching degree and the density of functional group application. Too high SED may cause excessive etching of the fiber surface, causing mechanical damage; too low SED makes it difficult to break the inert layer on the carbon fiber surface. By precisely controlling SED, a balance between surface activation and structural integrity can be achieved, ensuring that the interface bonding strength between the subsequent coating and the fiber is improved. This parameter is the core indicator of process repeatability and is used to guide the consistency control of different batches of fabric processing. This process breaks the inertness of the fiber surface and provides a physical anchoring and chemical bonding basis for the firm bonding of the subsequent nano-hybrid coating.

Preparation and Properties of Nano-SiO_2-Epoxy Hybrid Reinforced Coatings

Tetraethyl orthosilicate (TEOS) is dissolved in anhydrous ethanol, and an appropriate amount of deionized water and hydrochloric acid catalyst are added. The solution is hydrolyzed and polycondensed in a water bath at 60°C to form a SiO_2 sol. The reaction process is controlled by the following sol-gel reaction:

$$Si(OR)_4+2H_2O \xrightarrow{H^+} SiO_2+4ROH \quad (2)$$

In Formula (2), R is an ethyl group. The reaction rate is regulated by pH and temperature. Acidic conditions inhibit excessive gelation and ensure the stability of the sol. The obtained SiO_2 sol is mixed with bisphenol A epoxy resin in a predetermined ratio. The molar ratio of TEOS/H_2O/EtOH was 1:4:40, and the mass ratio of epoxy/curing agent/accelerator was 100:85:2. The coating thickness, controlled by the dip-pull speed, was approximately 15±2 μm. DSC analysis confirmed a curing conversion rate exceeding 95%. Methyltetrahydrophthalic anhydride, a curing agent, and a small amount of accelerator benzyldimethylamine are added. The mixture is mechanically stirred at 40°C until a uniform hybrid prepreg is formed. The prepreg is evenly coated on the surface of the plasma-treated carbon fiber fabric by the dip-pull method. The pull-up speed is controlled by a precision transmission system to ensure the consistency of the coating thickness. After coating, the sample is placed in a gradient heating oven and cured at 60°C for 2h and then at 120°C for 1h to complete the cross-linking reaction. The hybrid coating forms a dense transition layer through the synergistic effect of SiO_2 nanoparticles and epoxy network, improves the stress transfer

ability between the fabric and the cement matrix, and inhibits the interface degradation in alkaline environment.

Integrated Intelligent Hybrid Conductive Mesh Weaving with Both Reinforcement and Sensing Functions

Stainless steel fibers with a diameter of 50μm and carbon fiber bundles are fed into the loom in parallel according to a preset ratio using a plain weaving process. The conductive mesh structure is formed by warp and weft interweaving. The warp density and weft density are controlled by the steel reed to ensure uniform fabric surface density [20]. The stainless steel fibers are continuously arranged along the force direction to form a conductive path, and the carbon fibers provide the main load-bearing function. The two are synchronously tensioned during the weaving process to avoid structural distortion due to elongation differences. After weaving, the fabric is subjected to pre-tension shaping treatment to eliminate internal stress and ensure that the conductive network and the reinforcement phase are deformed in coordination during the subsequent composite process. To quantify the conductive stability of the conductive mesh, the unit area resistivity ρ_s is defined as follows:

$$\rho_s = R_1 \cdot \frac{w}{L} \tag{3}$$

In Formula (3), R_1 is the measured inter-electrode resistance; w is the conductive path width; L is the electrode spacing. This parameter reflects the in-plane uniformity of the fabric's conductive properties and is used to evaluate the control level of fiber contact resistance and continuity during the blending process.

In the weaving process of stainless steel fiber blended conductive mesh, to control the balance between the continuity of the conductive path and mechanical interference, the fiber volume fraction V_f is defined as follows:

$$V_f = \frac{\frac{G_f}{\rho_f}}{\frac{G_f}{\rho_f} + \frac{G_m}{\rho_m}} \tag{4}$$

In Formula (4), G_f is the mass of the reinforcing fiber per unit area; G_m is the mass of the matrix or supporting fiber per unit area; ρ_f and ρ_m are the densities of the fiber and matrix materials, respectively. This parameter determines the percolation threshold and mechanical contribution ratio of the conductive network and is the core basis for the design of the blended structure. By controlling V_f, it is ensured that the stainless steel fiber reaches the conductive percolation threshold while not excessively weakening the fabric's flexibility and drapeability.

The physical integration of mechanical enhancement and electrical response is achieved through structural design, providing a stable signal transmission foundation for subsequent self-sensing functions.

Matrix Preparation of Tough Cement-based Permeable Composite Materials (FRCM)

The matrix dry material is prepared by using silicate cement and fine sand in a mass ratio of 1:2.5. The water-cement ratio is determined by rheological control. 15% PVA (Polyvinyl Alcohol) emulsion (based on cement mass) is added as a polymer modifier to improve the toughness and bonding properties of the matrix. The 15% dosage was optimized through preliminary tests; it significantly improves crack resistance and interfacial bond strength, with compressive strength maintained at >90% of the control group, making it suitable for the modified FRCM matrix. A water reducer (polycarboxylic acid series) is added to the mixing water at a fixed dosage. After stirring evenly, the dry material is added in batches and mechanically stirred for 3 minutes until the slurry is uniform and free of agglomerates. The application of PVA emulsion improves the interface transition zone structure between cement hydration products and fibers. Its film-forming properties help to seal micropores and inhibit crack propagation. To evaluate the matrix's ability to penetrate fibers, the capillary permeability coefficient K_c is defined as follows:

$$K_c = \frac{m(t)}{A\sqrt{t}} \tag{5}$$

In Formula (5), $m(t)$ is the mass of slurry absorbed within the penetration time t, and A is the contact area. This parameter reflects the penetration dynamics of the slurry in the textile mesh and directly determines the impregnation adequacy of the fiber bundle and the interlayer bonding quality. After the slurry

is prepared, it is used for fabric impregnation immediately to ensure that the composite layer is formed before initial setting to avoid an increase in void content due to a decrease in fluidity.

PREPARATION OF MULTIFUNCTIONAL REINFORCED SPECIMENS AND COUPLED ENVIRONMENT DURABILITY EXPERIMENTAL PLAN

A C30 concrete beam measuring 150mm × 150mm × 600mm is prepared as the base component. After 28 days of standard curing, the tensile surface is sandblasted to ISO Sa2.5 to remove laitance and oil contamination, resulting in a standardized, clean, rough interface and ensuring consistent initial bonding with the reinforcement layer. A carbon fiber fabric activated by plasma and coated with a nano-SiO_2-epoxy hybrid coating and a stainless steel fiber hybrid mesh are used as reinforcement layers. Three layers are sequentially adhered to the bottom surface of the beam. A modified cement-based FRCM material is evenly applied between each layer, with a total composite thickness of 5mm. The Modified FRCM matrix uses a water-cement ratio of 0.45, with 15% PVA emulsion (by cement mass) and a polycarboxylic acid superplasticizer at 1.2% by dry weight. This layered molding process is designed to optimize fabric infiltration and minimize interlaminar defects. After molding, the beam is cured under standard conditions for 14 days to fully hydrate the cement matrix and achieve design strength.

While carbonation and freeze-thaw cycles are also critical degradation factors for concrete, they were not included in this specific test to isolate the impact of moisture and thermal stress on the fiber-matrix interface. To evaluate the long-term service performance, an accelerated aging test is conducted using a 180-day temperature-humidity cycling regimen. The current aging protocol focuses on the synergistic effects of temperature and humidity fluctuations. Each cycle consists of two phases: (1) a high-temperature, high-humidity phase at 60°C and 85% RH for 6 hours, followed by (2) a low-temperature, low-humidity phase at 10°C and 30% RH for 6 hours, completing a 12-hour cycle. These experimental conditions simulate the coupled degradation effects of temperature and humidity fluctuations on interfacial adhesion, matrix integrity, and conductive network stability in harsh environments, enabling rapid assessment of durability. The interfacial bond strength was measured using a single-lap shear test (per ASTM D3165) on a universal testing machine, with the degradation rate calculated as the percentage decrease in average bond strength after aging. While ASTM D3165 is typically used for polymer adhesive joints, it was employed here to

specifically evaluate the fiber-matrix interfacial strength of the coated carbon fiber bundles under controlled conditions. This approach isolates the effect of the nano-modified coating. For a more comprehensive assessment of the system-level bond performance with concrete, future work will conduct validation tests following the RILEM TC 232-TDT protocol. After aging, all specimens are subjected to four-point bending loading on a 200 kN universal testing machine at a loading rate of 0.5 mm/min. Mid-span deflection is recorded using displacement sensors, and load-displacement curves are simultaneously collected to analyze mechanical properties such as load-bearing capacity, stiffness, and ductility. During loading, a digital multimeter is used to monitor the resistance change of the stainless steel fiber network in real-time at a sampling rate of 1 Hz. This approach aims to simultaneously acquire mechanical and electrical signals, thereby establishing a correlation between the electrical response and structural deformation and verifying the feasibility of the self-sensing function. After the test, combined with crack development images and failure morphology, the reinforcement system's structural enhancement efficiency, bond stability, self-sensing responsiveness, crack suppression capability, and overall performance retention are systematically evaluated.

To systematically evaluate the impact of different material configurations on reinforcement performance, the experimental design includes various fabric combinations and interface treatments. Specific specimen parameters are shown in Table 1, where CF stands for Carbon Fiber, and SSF stands for Stainless Steel Fiber.

Table 1. Specimen design and material configuration parameters

Specimen number	Fabric type	Mixed ratio (CF:SSF)	Coating type	FRCM layers	Matrix type	Aging treatment
RC	-	-	-	-	-	-
TRC-1	CF	100:0	-	3	Cement mortar	-
TRC-2	CF	100:0	SiO_2-epoxy	3	Cement mortar	-

TRC-3	CF+SSF	75:25	SiO_2-epoxy	3	Modified FRCM	-
TRC-4	CF+SSF	75:25	SiO_2-epoxy	3	Modified FRCM	180-day temperature and humidity cycle

Table 1 lists the fiber type, carbon fiber to stainless steel fiber ratio, nano-modified coating, number of FRCM layers, substrate material type, and whether or not the specimens underwent temperature-humidity cycling aging. This demonstrates the control of experimental variables and reflects a multi-factor comparative design, supporting the credibility of subsequent analysis.

For each material configuration listed in Table 1, a total of five replicate specimens were prepared for flexural testing to ensure statistical robustness. The unreinforced concrete control group and the reinforced groups (TRC-1 to TRC-4) were all subjected to the same four-point bending loading protocol with a displacement rate of 0.5 mm/min until failure. The GF is calculated as $GF = (\Delta R/R_o)/\varepsilon$, where ΔR is the resistance change measured by a digital multimeter, R_o is the initial resistance, and ε is the strain obtained from a high-precision extensometer attached to the composite surface.

The performance testing process relies on a high-precision measurement system to ensure data reliability. All tests are conducted using a standardized measurement system. The equipment and parameter configurations used are shown in Table 2.

Table 2. Test system and measurement parameter configuration

Measurement items	Equipment	Model/Specifications	Range	Accuracy	Sampling frequency	Installation location/method
Load	Universal testing machine	WAW-200E	200 kN	±0.5% FS	1 Hz	Vertical loading head

Deflection	Displacement sensor	LVDT-10 mm	10 mm	±0.01 mm	1 Hz	mid-span bottom
Crack width	Digital Image correlation system	DIC-3D	—	0.01 mm	5 Hz	Full-field scanning of the beam side surface
Resistance change	Digital multimeter	Keithley 2700	200 Ω	0.001 Ω	1 Hz	Stainless steel fiber electrode connection at both ends
Environmental conditions	Temperature and humidity recorder	HOBO UX100	- 20~70 °C, 0~100% RH	±0.35 °C, ±2% RH	10 minutes/time	Inside the aging chamber

Table 2 specifies the technical parameters, including the equipment model, range, accuracy, and sampling frequency, for measuring load, deflection, crack width, resistance change, and ambient temperature and humidity. This ensures the quality of simultaneous monitoring of structural responses and functional signals.

COMPOSITE REINFORCEMENT SYSTEM PERFORMANCE TESTING AND MECHANISM ANALYSIS

Flexural Capacity

The core goal of building structural reinforcement is to improve the load-bearing capacity of components. The mechanical contribution of textile-reinforced composites depends on fiber orientation, interfacial transfer efficiency, and matrix synergy. The impact of different material configurations on the flexural performance of beams must be quantified through standardized loading tests to clarify the actual contribution of each modification step to structural reinforcement. The results of structural reinforcement efficiency are shown in Figure 2.

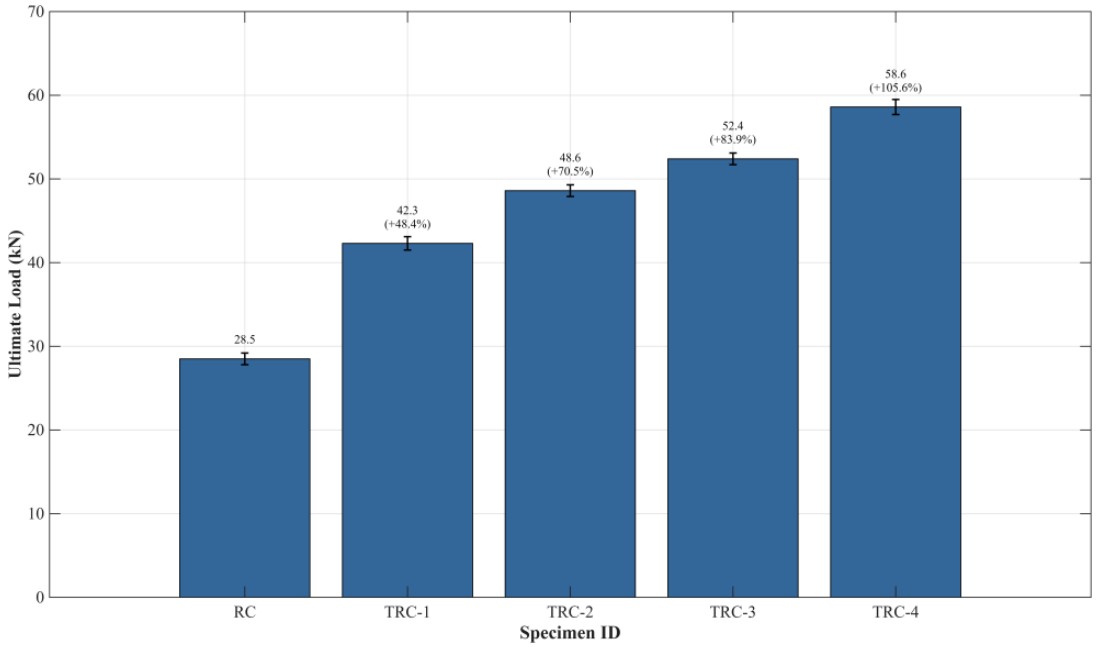

Figure 2. Comparison of ultimate flexural capacity of specimens

In Figure 2, the horizontal axis represents the specimen number, including RC (Reinforced Concrete), TRC-1, TRC-2, TRC-3, and TRC-4, while the vertical axis represents the ultimate flexural capacity, reflecting the structural reinforcement efficiency of each reinforced beam. The average bearing capacity of the RC specimens is 28.5 kN, serving as the baseline. TRC-1 increases this to 42.3 kN, a 48.4% increase. TRC-2, after the application of a nano-modified coating, further increases this to 48.6 kN, a 70.5% increase. TRC-3, using a hybrid conductive mesh and a modified matrix, reaches 52.4 kN, an 83.9% increase. After integrating all improvements, TRC-4 reaches 58.6 kN, a 105.6% increase over the baseline. Error bars above each column represent standard deviations and are all less than 1.0 kN, demonstrating good data reproducibility. The bearing capacity shows a gradual upward trend from RC to TRC-4, indicating a cumulative enhancement effect from plasma treatment, nano-SiO_2-epoxy coating, stainless steel fiber blending, and matrix modification. The highest bearing capacity of TRC-4 demonstrates that multi-scale interface manipulation and functional integration can effectively improve the overall mechanical properties of textile composite reinforcement systems, validating the effectiveness of this approach for structural reinforcement.

Evolution of Interface Bond Performance Before and After Hygrothermal Aging

The bond between fabric and concrete determines effective load transfer. Bond degradation under long-term environmental conditions is the primary cause of reinforcement failure. Evaluating the performance retention of different interface designs after hygrothermal cycling is a key step in verifying material durability. The evaluation results are shown in Figure 3.

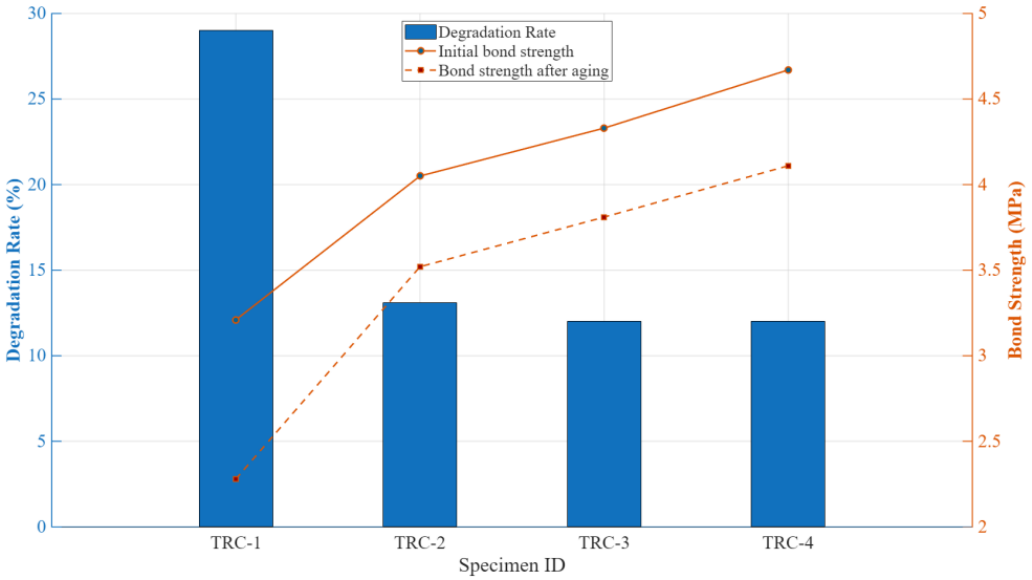

Figure 3. Comparison of interfacial bond strength and degradation rate before and after aging

In Figure 3, the horizontal axis represents specimen number; the left vertical axis represents degradation rate, and the right vertical axis represents interfacial bond strength. TRC-1 has an initial bond strength of 3.21 MPa, which decreases to 2.28 MPa after aging, with a degradation rate of 29.0%. After the application of the nano-modified coating, TRC-2's initial strength increases to 4.05 MPa, which decreases to 3.52 MPa after aging, with a degradation rate of 13.1%. TRC-3 and TRC-4 have initial strengths of 4.33 MPa and 4.67 MPa, respectively, and their degradation rates stabilize at 12.0% after aging, demonstrating excellent durability. With the application of the nano-hybrid coating and modified matrix, the bond strength gradually increases, and the degradation rate decreases significantly. TRC-1, without interfacial modification, experiences significant performance degradation, while TRC-2 through TRC-4, with their multiple protection designs,

significantly improve interfacial stability. Data shows that the nano-SiO_2-epoxy coating effectively inhibits erosion of the fiber-matrix interface in hot and humid environments, and the optimized hybrid structure and matrix further enhance the interface's resistance to degradation. The superior performance stems from the SiO_2 nanoparticles' ability to densify the interfacial transition zone and form additional C-S-H gel, while the epoxy resin provides a flexible, hydrophobic barrier against moisture ingress. This trend validates the critical role of multi-scale interface control strategies in improving the long-term bond stability of textile composites, providing a reliable basis for the application of functional reinforcement materials in complex environments.

Strain Response Sensitivity and Stability of Self-Sensing Function

Functional composites must not only possess load-bearing capacity but also be able to reflect changes in the internal state of the structure. The correlation between the resistance signal and mechanical deformation can be used to evaluate the self-sensing performance, and its linearity and stability directly determine the reliability of the monitoring system. The corresponding verification results of the self-sensing function are shown in Figure 4.

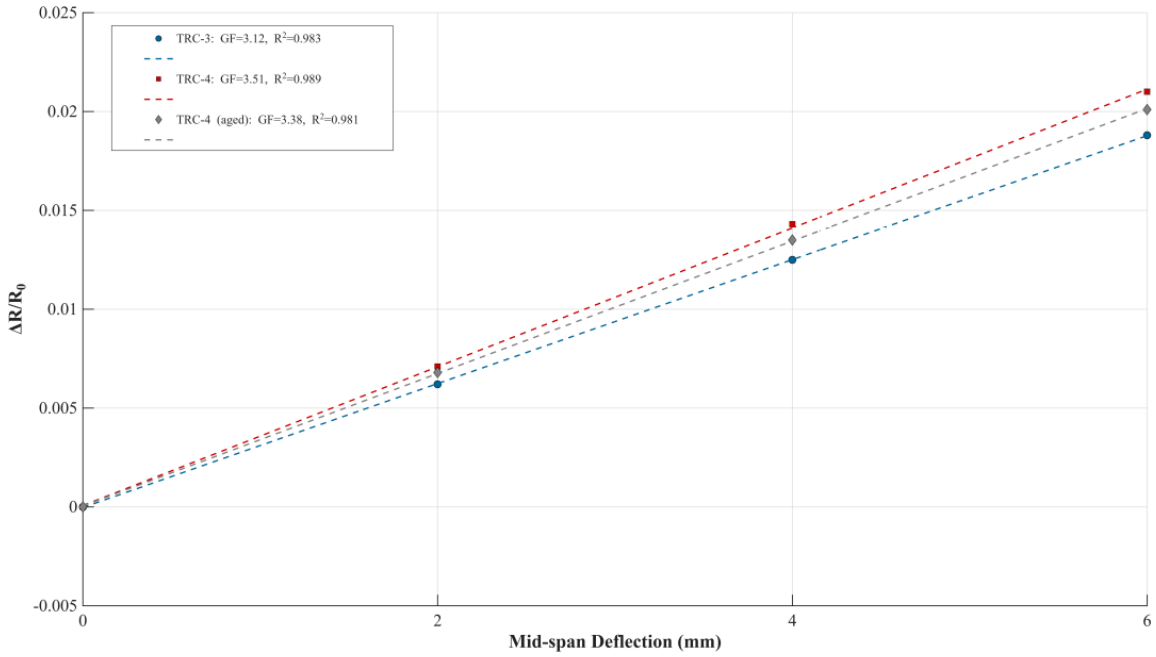

Figure 4. Correspondence between resistance response and structural deformation

In Figure 4, the horizontal axis represents the mid-span deflection, which is the bending deformation of the component after being subjected to force; the vertical axis represents the relative change in resistance ($\Delta R/R_o$), which reflects the response characteristics of the self-sensing function. Over a deflection range of 0–6.0 mm, the $\Delta R/R_o$ of the TRC-3 increases from 0.0062 to 0.0188, with a linear fit slope (GF) of 3.12 and R^2=0.983. The response of the TRC-4 is even more pronounced, reaching a $\Delta R/R_o$ of 0.0210, a GF of 3.51, and an R^2=0.989, indicating a higher sensitivity of the hybrid conductive mesh. The aged TRC-4 maintains a good linear response at the same deformation with a $\Delta R/R_o$ of 0.0201, a GF of 3.38, and an R^2=0.981. All three datasets show a highly linear relationship, with the signal increasing steadily with structural deformation without abrupt changes or interruptions. A GF value exceeding 3.0 indicates that the stainless steel fiber network possesses excellent piezoresistive properties, enabling real-time capture of structural strain development. While sensitivity decreased slightly after aging, the GF value reaches 3.38, indicating that the nano-modified interface effectively protects the stability of the conductive pathway. The GF value of 3.38 was calculated from the linear fit (R^2=0.981) of resistance change vs. deflection over a 0–6.0 mm range for aged TRC-4 specimens, with individual measurements showing a mean GF of 3.38 and a standard deviation of ±0.07 across five tests. The data shows consistent patterns of change, with no signal drift or failure. This demonstrates that the constructed self-sensing system possesses reliable strain monitoring capabilities under long-term service conditions, providing continuous feedback on the structural health status.

Evaluation of Crack Extension Control Effectiveness

Crack initiation and extension are important indicators of damage evolution in concrete structures. An effective reinforcement system should delay the formation of primary cracks and promote the distribution of multiple cracks. By recording the evolution of maximum crack width as a function of load, the material's ability to restrain crack behavior can be intuitively assessed. The variation of maximum crack width in the specimens as a function of load is shown in Figure 5. The maximum crack width was extracted from the Digital Image Correlation (DIC) system by identifying the peak strain value along the primary crack path and converting it to physical displacement based on the calibrated scale.

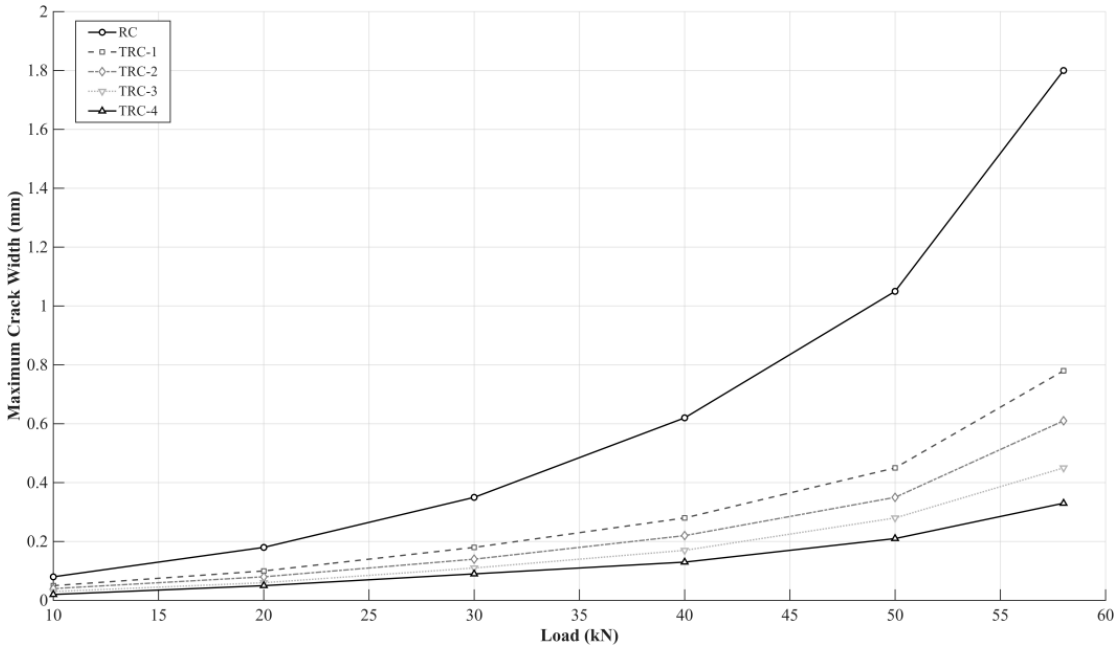

Figure 5. Changes in maximum crack width of each specimen as a function of load

The horizontal axis in Figure 5 represents the applied load, and the vertical axis represents the maximum crack width, reflecting the crack growth behavior of different specimens during loading. The crack width of the RC specimen reaches 1.05mm at 50kN, increasing to 1.80mm at 58kN, demonstrating rapid crack expansion. Under the same load, the crack widths of the TRC-1 specimen are 0.45mm and 0.78mm, respectively; 0.35mm and 0.61mm for TRC-2; 0.28mm and 0.45mm for TRC-3; only 0.33mm at 58kN for TRC-4, significantly lower than the other groups. From 10kN to 58kN, the crack growth rate of the TRC-4 specimen is significantly lower than that of the RC specimen, demonstrating a significant crack suppression effect. With the application of nano-modified coatings, hybrid conductive meshes, and modified substrates into the material system, the crack width gradually decreases, and the crack expansion trend becomes more gradual. The TRC-4 maintains numerous, fine microcracks under peak load, with no rapid penetration of the main cracks. This indicates that the fibers effectively bridge the cracks, delaying damage concentration. These data demonstrate that the constructed multifunctional composite material not only enhances load-bearing capacity but also effectively improves the crack control properties of concrete, enhancing the durability and service safety of the structure, verifying its superiority in suppressing crack growth.

Mechanisms of Long-Term Performance Degradation under Multi-Factor Coupling

Actual service environments are often characterized by the coupling of multiple degradation factors, making a single performance metric inadequate for fully reflecting a material's long-term performance. A multi-dimensional evaluation system is constructed to reveal the overall stability differences between different design schemes under complex conditions. The performance retention comparison results for each specimen are shown in Figure 6.

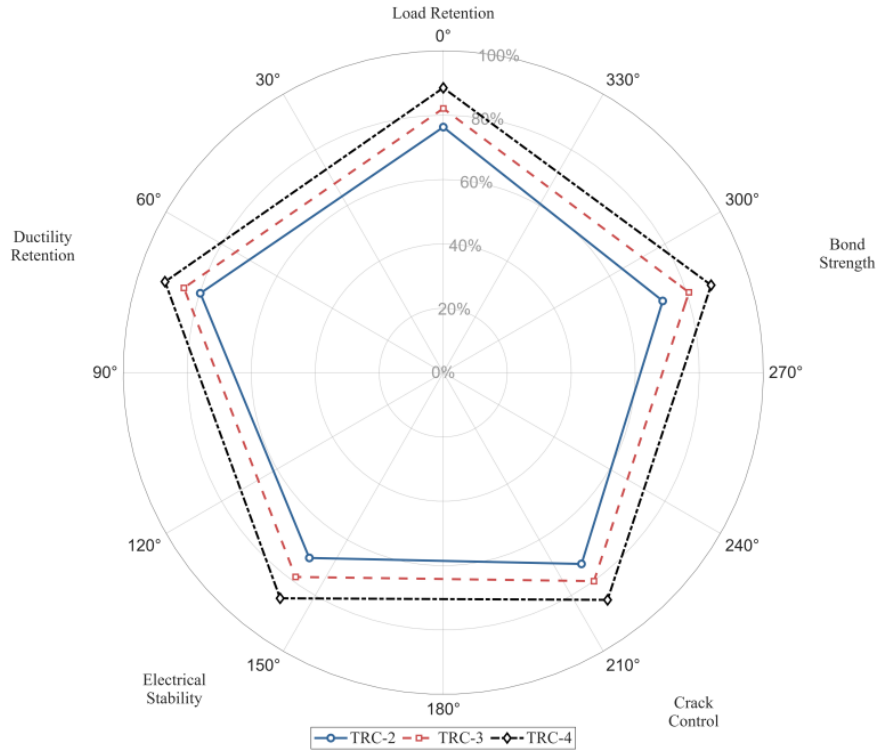

Figure 6. Comparison of comprehensive performance retention of specimens under complex environments

The comprehensive performance retention index (CPR) in Figure 6 is calculated as a weighted sum of five normalized metrics: Load Retention (P1), ductility (P2), electrical stability (P3), crack control (P4), and bond strength (P5). The formula is: CPR = w1*P1 + w2*P2 + w3*P3+ w4*P4+ w5*P5. The weights (w1=0.3, w2=0.2, w3=0.2, w4=0.2, w5=0.1) were determined by the Analytic Hierarchy Process (AHP) based on expert assessment.

Figure 6 shows a comparison of the comprehensive retention rates of five key properties for three specimens after 180 days of temperature-humidity cycling aging. The five dimensions are: load-bearing capacity

retention, ductility retention, electrical stability, crack control, and bond strength retention. These are evenly distributed along the five axes of the radar chart. The retention rates of TRC-2 are 76.3%, 79.8%, 71.2%, 73.5%, and 72.1%, respectively, with the smallest profile and limited overall performance retention; those of TRC-3 are 82.1%, 85.2%, 78.5%, 80.1%, and 80.7%, respectively, with a significantly expanded profile, indicating that all performances have been improved; TRC-4 performs best in all indicators, at 88.5%, 91.4%, 86.7%, 87.3%, and 88.0%, respectively, indicating that it has the strongest ability to synergistically retain multiple properties. From TRC-2 to TRC-4, the profile area gradually expands, reflecting that the synergistic effect of the nano-modified coating, the mixed conductive mesh, and the modified matrix improves the comprehensive durability of the material in a complex coupling environment. The data is evenly distributed with no obvious shortcomings, verifying that the proposed multifunctional composite system is not only optimized in terms of a single performance, but also achieves a systematic improvement in the long-term stability of the structure-function integration.

Comparison with State-of-the-Art Technologies

To position our work within the current state-of-the-art, we compare the key performance metrics of our smart textile-reinforced composite system with three representative technologies: (1) Conventional Textile-Reinforced Concrete (TRC), (2) Epoxy-coated CFRP Plates, and (3) CNT-based Self-Sensing Composites. As summarized in Table 3, our system demonstrates a superior balance of strength enhancement, durability, and self-sensing capability.

Table 3. Performance Comparison with Representative Technologies

Technology	Flexural Strength Improvement	Interfacial Degradation after Aging	Gauge Factor (GF)	Scalability
Conventional TRC	~80%	High (>30%)	N/A	High
Epoxy-coated CFRP [21]	>90%	Moderate (~20%)	N/A	Medium
CNT-based Composite [22]	~70%	Low (<10%)	~1.5	Low
This Work	>105%	Low (12%)	>3.38	High

Table 3 shows that our approach achieves a higher flexural strength improvement (>105%) compared to conventional TRC (~80%), while addressing the long-term durability issues of epoxy-coated CFRP plates in wet environments. Furthermore, it offers a significantly higher Gauge Factor (GF > 3.38) than CNT-based composites (GF ~ 1.5), indicating superior sensing sensitivity. This comparison highlights that our multi-scale design strategy successfully integrates high performance, long-term stability, and robust self-sensing into a single, practical solution.

CONCLUSIONS

This paper constructs a multifunctional textile-reinforced composite system combining a nano-modified interface with a hybrid conductive mesh, achieving simultaneous improvements in mechanical properties and functional response in building structural reinforcement. Plasma-activated carbon fiber fabric surfaces, combined with a SiO_2-epoxy hybrid coating to strengthen the bond between the fibers and the cement matrix, effectively inhibits bond degradation in hot and humid environments. A continuous conductive network is formed by hybridizing stainless steel and carbon fibers, integrated into the FRCM layer to achieve strain self-sensing. This study demonstrates that a plasma-activated, SiO_2-epoxy coated carbon fiber/stainless steel hybrid mesh enhances concrete flexural strength by over 105%, limits interface degradation to 12% after aging, and achieves a stable self-sensing Gauge Factor of 3.38 ± 0.07, providing a multifunctional solution for durable structural reinforcement. This approach transcends the limitations of traditional reinforcement materials with a single function, achieving an integrated design of reinforcement, durability, and sensing. Its innovation lies in the synergistic mechanism of multi-scale interface regulation and functional structural integration. However, the performance evolution under the coupled effects of long-term carbonization and fatigue requires further verification.

Author Contributions

Guohua Cheng designed, collected and analyzed the data, and drafted the manuscript. Guohua Cheng conducted the study, critically revised the manuscript for important intellectual content, and gave final approval of the version to be published. Guohua Cheng participated fully in the work, take public responsibility for appropriate portions of the content, and agreed to be accountable for all aspects of the

work in ensuring that questions related to the accuracy or integrity of any part of the work are appropriately investigated and resolved.

Conflicts of Interest

The author declares no conflict of interest.

Funding

This research received no external funding.

Acknowledgements

Not applicable.

REFERENCES

[1] Moy CKS, Revanna N. Experimental and DIC study of reinforced concrete beams strengthened by basalt and carbon textile reinforced mortars in flexure. Buildings. 2023; 13(7):1765. doi: 10.3390/buildings13071765

[2] Deng Z, Xia Q, Gong M, Xu J. Flexural Strengthening of Two-Way RC Slabs with Textile Reinforced Mortar: Experimental Study and Calculation Model. KSCE Journal of Civil Engineering. 2023; 27(12):5268-5280. doi: 10.1007/s12205-023-2174-6

[3] Karakasis IC, Papanicolaou CG, Triantafillou TC. Residual textile reinforced mortar-to-concrete bond after exposure to harsh environments. Structural Concrete. 2025; 26(3):3597-3610. doi: 10.1002/suco.202400421

[4] Verre S. Effect of different environments' conditioning on the debonding phenomenon in fi-ber-reinforced cementitious matrix-concrete joints. Materials. 2021; 14(24):7566. doi: 10.3390/ma14247566

[5] Alwis LSM, Bremer K, Roth B. Fiber optic sensors embedded in textile-reinforced concrete for smart structural health monitoring: A review. Sensors. 2021; 21(15):4948. doi: 10.3390/s21154948

[6] Chaudhary B, Winnard T, Oladipo B, Das S, Matos H. Review of Fiber-Reinforced Composite Structures with Multifunctional Capabilities through Smart Textiles. Textiles. 2024; 4(3):391-416. doi: 10.3390/textiles4030023

[7] Elnassar Z, Abed F, El Refai A, El-Maaddawy T. FRCM confinement of concrete columns: a review of strength and ductility enhancements. Composite Structures. 2025; 370:119389. doi: 10.1016/j.compstruct.2025.119389

[8] Askouni PD, Kapsalis P, Papanicolaou CG, Triantafillou TC. Strengthening of Masonry and Concrete Members with Textile-Reinforced Alkali-Activated Mortars: A Review on the Mechanical Performance. Materials. 2025; 18(7):1517. doi: 10.3390/ma18071517

[9] Wu C, Pan Y, Yan L. Mechanical properties and durability of textile reinforced concrete (TRC)-a review. Polymers. 2023; 15(18):3826. doi: 10.3390/polym15183826

[10] Karakasis IC, Papadakis VG, Papanicolaou CG, Triantafillou TC. Textile reinforced mortar (TRM) as a barrier for concrete structures subjected to carbonation and chloride attack: experimental investigation and analytical modeling. Materials and Structures. 2024; 57(2):37. doi: 10.1617/s11527-024-02303-3

[11] Escobar KI, Oller E, Murcia-Delso J, Carrasco LF. Mechanical characterization of hemp textile reinforced mortars for structural strengthening applications. Construction and Building Materials. 2025; 489:142256. doi: 10.1016/j.conbuildmat.2025.142256

[12] Preinstorfer P, El Kadi M, Dittel G, Ghiassi B, Müller S, Mansur de Castro Silva R, et al. Article of RILEM TC 292-MCC: bond behaviour of textile-reinforced concrete-a review. Materials and Structures. 2024; 57(4):97. doi: 10.1617/s11527-024-02339-5

[13] Joo JH, Kim SH, Yim YJ, Bae JS, Seo MK. Interfacial Interlocking of Carbon Fiber-Reinforced Polymer Composites: A Short Review. Polymers. 2025; 17(3):267. doi: 10.3390/polym17030267

[14] Elseady AAE, Zhuge Y, Ma X, Chow CW, Lee I, Zeng J. Self-sensing and piezoresistive performance of carbon fibre textile-reinforced cementitious composites under tensile loading. Composite Structures. 2025; 356:118897. doi: 10.1016/j.compstruct.2025.118897

[15] Elseady AAE, Zhuge Y, Ma X, Chow CW, Lee I, Zeng J, et al. Development of self-sensing cementitious composites by incorporating a two-dimensional carbon-fibre textile network for structural health moni-

toring. Construction and Building Materials. 2024; 415:135049. doi: 10.1016/j.conbuildmat.2024.135049

[16] Singh S, Kamble Z, Neje G. Electro-mechanical behavior of self-sensing textile-reinforced composites for in situ structural health monitoring. Journal of Reinforced Plastics and Composites. 2024; 43(21-22):1205-1213. doi: 10.1177/07316844231202370

[17] Kumar S, Jayanarayanan K, Balachandran M. High-performance thermoplastic polyarylether-ketone/carbon fiber composites: comparison of plasma, carbon nanotubes/graphene nano-anchoring, surface oxidation techniques for enhanced interface adhesion and properties. Composites Part B: Engineering. 2023; 253:110560. doi: 10.1016/j.compositesb.2023.110560

[18] Eyckens DJ, Jarvis K, Barlow AJ, Yin Y, Soulsby LC, Wickramasingha YA, et al. Improving the effects of plasma polymerization on carbon fiber using a surface modification pretreatment. Composites Part A: Ap-plied Science and Manufacturing. 2021; 143:106319. doi: 10.1016/j.compositesa.2021.106319

[19] Sampino S, Ciardiello R, D'Angelo D, Cagna L, Paolino DS. Effect of the atmospheric plasma treatment pa-rameters on the surface and mechanical properties of carbon fabric. Materials. 2024; 17(11):2547. doi: 10.3390/ma17112547

[20] Hasan KMF, Horváth PG, Alpár T. Potential fabric-reinforced composites: a comprehensive review. Journal of Materials Science. 2021; 56(26):14381-14415. doi: 10.1007/s10853-021-06177-6

[21] Sharma H, Kumar A, Rana S, Guadagno L. An overview on carbon fiber-reinforced epoxy composites: effect of graphene oxide incorporation on composites performance. Polymers. 2022; 14(8):1548. doi: 10.3390/polym14081548

[22] Koutsotolis L, Karalis G, Itskaras AV, Tsirka K, Paipetis AS. A carbon nanotube-based thermoelectric generator integrated into a smart composite for structural health monitoring. Materials Research Express. 2024; 11(4):045705. doi: 10.1088/2053-1591/ad3b68